Intra-operative point-of-procedure delineation of oral cancer margins using optical coherence tomography

Sumsum P. Sunny[a,b], **Sagar Agarwal**[a], **Bonney Lee James**[b], **Emon Heidari**[c], **Anjana Muralidharan**[b], **Vishal Yadav**[a], **Vijay Pillai**[a], **Vivek Shetty**[a], **Zhongping Chen**[c], **Naveen Hedne**[a], **Petra Wilder-Smith**[c], **Amritha Suresh**[a,b], **Moni Abraham Kuriakose**[a,b,*]

[a]Head and Neck Oncology, Mazumdar Shaw Medical Centre, NH Health City, Bangalore, India

[b]Integrated Head and Neck Oncology Program (DSRG-5), Mazumdar Shaw Medical Foundation, NH Health City, Bangalore, India

[c]Beckman Laser Institute, UCI, Irvine, USA

Abstract

Objectives: Surgical margin status is a significant determinant of treatment outcome in oral cancer. Negative surgical margins can decrease the loco-regional recurrence by five-fold. The current standard of care of intraoperative clinical examination supplemented by histological frozen section, can result in a risk of positive margins from 5 to 17 percent. In this study, we attempted to assess the utility of intraoperative optical coherence tomography (OCT) imaging with automated diagnostic algorithm to improve on the current method of clinical evaluation of surgical margin in oral cancer.

Materials and methods: We have used a modified handheld OCT device with automated algorithm based diagnostic platform for imaging. Intraoperatively, images of 125 sites were captured from multiple zones around the tumor of oral cancer patients (n = 14) and compared with the clinical and pathologic diagnosis.

Results: OCT showed sensitivity and specificity of 100%, equivalent to histological diagnosis (kappa, $\kappa = 0.922$), in detection of malignancy within tumor and tumor margin areas. In comparison, for dysplastic lesions, OCT-based detection showed a sensitivity of 92.5% and specificity of 68.8% and a moderate concordance with histopathology diagnosis ($\kappa = 0.59$). Additionally, the OCT scores could significantly differentiate squamous cell carcinoma (SCC) from dysplastic lesions (mild/moderate/severe; $p < 0.005$) as well as the latter from the non-dysplastic lesions ($p < 0.05$).

Conclusion: The current challenges associated with clinical examination-based margin assessment could be improved with intra-operative OCT imaging. OCT is capable of identifying

microscopic tumor at the surgical margins and demonstrated the feasibility of mapping of field cancerization around the tumor.

Keywords

Introduction

Surgery is the primary treatment modality in management of oral cancers. Adequate surgical margin is one of the most important prognostic factors that determine disease outcome, with involved margin lowering the loco-regional control by five folds [1–3]. The standard surgical treatment involves tumor resection with a cuff of clinically normal tissue beyond the macroscopic tumor margin in an attempt to achieve microscopic tumor clearance. Given the need of a minimum of 5 mm pathological clearance and accounting for 30% tissue shrinkage due to formalin fixation, a 1 cm margin is the current standard adopted during surgical excision of oral cancer [4]. The intraoperative clinical evaluation may be supplemented by histological frozen section evaluation. However, this process is time consuming and the tissue processed cannot be revaluated by conventional histopathology. Even with frozen section evaluation, 5–17% of surgical resections can have positive surgical margins [2,5]. Several imaging modalities such as ultrasonography [6] and auto-fluorescence [7] have been attempted for the delineation of tumor margin, however none have gained widespread clinical use. Field cancerization refers to the lateral spread of tumors due to progressive transformation of cells adjacent to tumor rather than the spread and invasion of adjacent epithelium by preexisting tumor [8]. The presence of this field effect poses a significant risk for cancer recurrence and progression even after removal of primary tumors [9]. An intra-operative, point-of-procedure diagnostic tool for the delineation of tumor margin and evaluation of the field cancerization effect is a clinical need, which may in turn lower the incidence of involved surgical margins and possibly improve disease outcome.

Optical coherence tomography (OCT) is a non-invasive modality with high-resolution microstructural imaging that maps the mucosal epithelium. The technology uses near infrared light and is widely used in the field of ophthalmology. OCT has been used in ex-vivo margin evaluation in oral squamous cell carcinoma patients, which suggested that OCT-based imaging could be used for tumor margin delineation [10]. We postulate that intraoperative OCT with automated diagnostic algorithm can improve accuracy of surgical margin delineation as compared to the current method of clinical and frozen section evaluation carried out during oral cancer excision surgery. Herein, we demonstrate the accuracy of intraoperative OCT with automated diagnostic algorithm to delineate the extent of field-cancerization during surgical excision of oral cavity cancers and its clinical efficacy to determine intra-operative tumor margin status.

Materials and methods

Study population and design

The study was designed (Fig. 1) as a prospective pilot study that attempted to evaluate the feasibility of intra-operative OCT to delineate surgical margins in patients undergoing surgery for oral squamous cell carcinoma (OSCC). The study was approved by the institutional ethics committee (NHH/MEC-CL-2015–279) and subjects were recruited during a two-month period (September to October 2016) after obtaining written informed consent.

The subjects reporting to Head and Neck Oncology service, Mazumdar Shaw Medical Center, Narayana Health, Bangalore, India with newly diagnosed OSCC were accrued for the study. The inclusion criteria were (i) subjects who were > 18-year-old (ii) histopathologically confirmed OSCC, and (iii) who consented to the study protocol. The exclusion criteria were (i) previous history of OSCC, (ii) subjects who have undergone previous anti-cancer therapy other than biopsy for the index tumor (iii) mouth opening less than 3 cm. The demographics, clinical and pathological details are summarized in Table 1.

After induction of anesthesia, the operating surgeon clinically evaluated the lesion and demarcated the intended surgical margins using an indelible marking pen, which is at least 1 cm away from the tumor induration. OCT images were captured intraoperatively from five different zones as shown in Fig. 1b. These zones constituted regions within tumor (Zone 1), tumor margin (Zone 2), surgical margin (Zone 3; 1cm from the clinical tumor margin), more than 1 cm away from surgical margin (Zone 4; > 2 cm from the clinical tumor margin), and contralateral side mucosa (Zone 5). Separate images were obtained from at least two different quadrants within each of the zones. Punch biopsies were performed from each of the imaged sites for histopathological correlation. The biopsy specimens were reported by pathologist according to WHO criteria [11,12]. The pathologist was blinded from the clinical and OCT diagnosis. Histopathology diagnosis was considered as the gold standard (reference standard) for comparison with clinical (current standard of care) and OCT diagnosis (index test). The extent of surgical margin was determined by clinical evaluation by the surgeon, assisted by frozen-section when indicated. The OCT imaging data was blinded to the operating surgeon. Every field which underwent interrogation by clinical, OCT imaging and histopathology was designated as normal, oral potentially malignant lesion (OPML) or malignant lesion.

OCT device and algorithm-based OCT score

The in-vivo OCT images were acquired using SD-OCT system (Supplementary Fig. 1A) [13] with the prototype 1-D scanning long probe (Supplementary Fig. 1B) [13]. The SD-OCT system using center wavelength of 930 nm has an axial resolution of 7.0 μm and lateral resolution of 15.0 μm. Using a 20 kHz, 1024-point CCD line-scan camera on the spectrometer detection arm, an imaging speed of 1.2 kHz was achieved (2 images per second) and image analysis takes 5–10 s for diagnosis depending on the size of the image field of view. A long rigid one pitch GRIN rod was used in this study to relay light from the proximal portion of the probe to the patient's tissue [13]. A MATLAB image processing

algorithm adopted from a previous study [14] was utilized to differentiate healthy and abnormal oral mucosa. Images were processed by the OCT system using an algorithm reported by our group earlier [13]. The OCT based algorithm assigned a neoplastic score, which stratified the lesion as non-dysplastic (−0.0918 to − 0.1280), dysplastic (−0.0780 to −0.0918) or malignant (−0.0580 to −0.0780) [13].

Statistical analysis

Sample size estimation: The minimum sample size was calculated for the diagnostic study [15]. Considering the alpha value of < 0.05 and power of 80% the minimum sample size required for the study is 78 sites [15]. We expected a drop out of 20% due to poor image quality and difficulty in imaging. The total sample size required is 94 sites in 14 patients (7 images per patient, not including contralateral normal). Therefore 14 patients were recruited in the study and 125 images were recorded.

Descriptive statistics were used to summarize details of patient demography, clinical features, and pathological diagnosis. Continuous variables were reported using median and interquartile range. Kolmogorv-Smirnov test was performed to assess the normal distribution of OCT scores and all statistical comparison between multiple groups were assessed by one-way-analysis of variance (ANOVA) using Kruskal-Wallis test. McNemar test was used to compare the proportions. The agreement between histopathology with OCT and visual/palpation diagnosis were examined using Kappa statistics [16,17]. P value < 0.05 (2 sided) is considered as significant. The sensitivity and specificity of OCT based diagnosis were calculated. All statistical analyses were done using Medcalc 14.8.1

Results

Clinical details of study population

A total of 125 images were captured from 14 patients, who were diagnosed with OSCC. The mean age of the patients was 55 years (range from 39 to 78). Twenty-eight percentage (n = 4) of patients were female and 72% (n = 10) were male with 93% (n = 13) of all patients having the history of tobacco use. The sites of the tumor were primarily buccal mucosa (44%, n = 6) with the other sites being alveolus (21%, n = 3), gingivo-buccal sulcus (14%, n = 2), tongue (14%, n = 2) and retro-molar-trigone (7%, n = 1). Majority of tumors were T4 (50%, n = 7) and T2 (36%, n = 5) lesions. The images (n = 120) captured included tumor (n = 13), tumor margins (n = 34), surgical margins (n = 35), > 1 cm surgical margin (n = 25) and the contralateral normal (n = 13) (Table 1).

OCT based diagnosis showed high correlation with histology

Among the 125 images, 120 were included in the analysis. Five images were excluded due to poor image quality. The details and distribution of the images based on the zones are provided in the study consort chart (Fig. 2). Histological evaluation (Supplementary Fig. 2) indicated that most of the sites were diagnosed as mild dysplasia (46%; n = 56); the others being SCC (20%; n = 24), moderate dysplasia (15%; n = 19) and severe dysplasia (4%; n = 5). Thirteen percent were non-dysplastic lesions (n = 16), wherein there was a clear demarcation of epithelium and connective tissue, however this structured architecture was

lost in SCC (Fig. 3). OCT diagnosis of neoplastic/dysplastic areas was comparable to histology in the tumor and tumor margin (zones 1–5) with excellent concordance (k = 0.83, CI = 0.73–0.93) (Fig. 4). Comparison between the OCT and histological diagnosis indicated that the OCT scores correlated with severity of the disease (Fig. 5). Kruskal-Wallis test showed significant difference among the groups; the OCT scores showed a range within each cohort and could differentiate SCC from non-dysplastic and dysplastic lesions (mild/moderate/severe; p   0.05) and dysplastic from non-dysplastic lesions (p   0.005).

A patient-wise analysis of the histology and OCT diagnosis showed that out of 14 patients, 57% (n = 8) showed SCC (11 fields) and/or severe dysplasia (5 fields) in tumor margins (Zone 2–4), all of which are detected by OCT accurately. In these eight patients, 38% (n = 3) of patients showed close margin (tumor in < 5 mm) in other sites after microscopic examination of completely excised tumor. Forty-three percentage (n = 6) showed no malignancy or severe dysplasia by OCT and histology (incisional biopsy) with *ex-vivo* microscopic examination also showing negative margins (> 0.5 cm).

Delineation of the malignant field by OCT

Tumor (Zone 1) and Tumor margins (Zone 2): Attempts were made to delineate the malignant and/or dysplastic field in these zones by OCT and visual examination. The results of which correlated with histopathology findings. Out of 47 sites (tumor, n = 13; tumor margin, n = 34), 49% (n = 23) were diagnosed as SCC, while 51% (n = 24) sites were dysplastic/non-dysplastic by histology. In comparison to the gold standard, OCT-based assessment showed a sensitivity and specificity of 100% (Table 2) in detection of malignant fields (SCC was considered as test positive and dysplastic/non-dysplastic lesion as test negative for efficacy evaluation). OCT score demonstrated excellent concordance with histology (κ = 0.92, CI = 0.82–1) in assessment of neoplastic/dysplastic areas. Clinical examination showed 100% specificity and 56.5% sensitivity (CI = 34.5–76.8), with poor concordance with histopathology (κ = 0.26, CI = 0.14–0.37). The low sensitivity was due to the under-diagnosis of malignant sites (n = 10) in the tumor margin (zone 2). McNeamer test shows significant difference between visual method (standard of care) and histopathology diagnosis (p = 0.0002).

Delineation of the dysplastic field by OCT

Surgical margins and contralateral sites (Zone 2 to Zone 5): Out of 80 histologically diagnosed dysplastic lesions in the margins and the contralateral sites, 92% (n = 74) were accurately diagnosed by OCT, while out of 16 non-dysplastic lesions (histopathological diagnosis), 69% (n = 11) sites were accurately diagnosed. For analysis, dysplastic lesions were considered as test positive and non-dysplastic lesions as test negative. The sensitivity and specificity for detection of dysplastic lesion by OCT were 92.5% (CI = 84.4–97.2) and 68.8% (11/16, CI = 49.3–89) respectively with moderate agreement with histopathology diagnosis (κ = 0.59; CI = 0.38–0.81). McNeamer test showed no significant difference between histopathology and OCT based diagnosis. Classification into grades showed that out of 80 lesions, 6% (n = 5), 24% (n = 19) and 70% (n = 56) were diagnosed as severe, moderate and mild dysplastic lesions respectively by histology. Among them, all severe and moderate dysplastic lesions (high-risk) [18] were

diagnosed as dysplasia by OCT. Eighty nine percentage (n = 50/56) of mild dysplasia were detected by OCT, while 11% of sites were designated as normal. Clinical examination diagnosed 24% (n = 19) of the dysplastic lesions as OPML.

Zone-wise assessment of field cancerization

Further, individual comparisons were carried out within each site of imaging around the tumor to document the accuracy of diagnosis of OCT in mapping the field of cancerization (Fig. 3).

Zone 1- Tumor (n = 13): OCT as well as clinical examination diagnosed all the sites in the tumor zone as malignant lesions accurately.

Zone 2-Tumor margin (n = 34): Histological evaluation diagnosed 30% of the biopsies as malignant (n = 10). OCT detected all malignant sites precisely, however, clinical diagnosis identified these sites as normal. A comparison of the dysplastic sites (64%, n = 22/34) in the tumor margin indicated that OCT diagnosed all of them accurately, while 32% (n = 11/34) were diagnosed as OPML and 68% (n = 23/34) as normal by clinical method. Among the images, 6% were non-dysplastic lesions (n = 2/34), which were accurately diagnosed by visual method but over-diagnosed by OCT imaging as dysplastic. The agreement between OCT and histology diagnosis in this zone was 0.876 (CI = 0.721–1).

Zone 3-Surgical margin, (n = 35): In the surgical margins, only 3% (1/35) was designated malignant by histology, which were accurately diagnosed as malignant by OCT but were considered normal by clinical examination. Majority of the sites were diagnosed as dysplastic lesion by histopathology (80%, 28/35), out of which 89% (n = 25/28) were diagnosed as dysplastic and 10% (n = 3/28) as normal by OCT. Clinical examination identified 21% (n = 6/28) and 79% (22/28) of the sites as OPML and normal respectively. Among the non-dysplastic lesions identified by histopathology (17%, n = 6/35), 67% (n = 4/6) were diagnosed accurately by OCT, while the remaining 33% (n = 2/6) were diagnosed as dysplastic. Clinical examination diagnosed all the non-dysplastic sites as normal. Kappa statistics indicated a good agreement between OCT and histology diagnosis (k = 0.60, CI = 0.27–0.92).

Zone 4- > 1 cm from surgical margin (n = 25): Beyond 1 cm from the surgical margin, 84% (n = 21/25) of the sites were dysplastic lesions by histopathology; out of these 96% (n = 20/21) were detected by OCT, while only 4% were detected (1/21) visually as OPML. Among the non-dysplastic sites (16%, n = 4/25), 75% (n = 3/4) were diagnosed accurately by OCT. All of them were deemed normal by visual diagnosis, while OCT over diagnosed 25% (n = 1/4) as dysplastic lesions. The agreement between histology and OCT diagnosis was 0.70 (CI = 0.31–1).

Zone 5-Contralateral mucosa (n = 13): 69% (n = 9) of contralateral sites were diagnosed dysplastic by histopathology. Of which, OCT detected 78% (n = 7/9) as dysplasia, while 11% (n = 1/9) were clinically diagnosed as OPML. All the non-dysplastic sites were

diagnosed accurately by OCT and clinical examination. The agreement between the OCT and histology diagnosis was 0.83 (0.34–1).

Discussion

Accurate demarcation of the surgical margin is critical for improving outcome of patients undergoing surgery for oral cancer. Surgical margin with 5 mm of histologically uninvolved mucosa is mandated by the current clinical guidelines [19]. Close (< 3mm) and positive margins propound poor prognosis [1,2]. The current practice of surgery guided by clinical examination by the surgeons and supplemented by frozen section histopathology is unable to offer consistent evaluation of surgical margins [2,5]. The sensitivity and specificity of frozen section in comparison to conventional histology is 72.7% and 93.9% respectively for oral cancer [20]. Given the need to improve the margin status post surgical resection, intra-operative imaging methods that reflect the 'microscopic' changes in the tumor-surrounding field could be of immense clinical utility. This study presents the first *in-vivo,* intraoperative, OCT-based real time imaging for delineation of tumor margin in patients undergoing surgery for oral cancer. The results suggest that OCT based diagnosis is equivalent to histology in detection of malignant/dysplastic fields with significant improvement over clinical examination, the current standard of care.

Imaging methods have been the major area of focus in intra-operative margin assessment in many cancers [21,22]. OCT has been proven effective in margin delineation of breast [21,22], skin [23] and vulva [24] malignancies reporting high sensitivity (90–100%) and specificity (80–92%). OCT combined with reflectance confocal microscopy showed 100% sensitivity in detection and depth assessment of basal cell carcinoma [25]. Label-free reflectance hyperspectral imaging with machine learning based classification showed 90% accuracy in tumor margin detection [26]. In oral cancer, OCT has been used for margin evaluation *ex-vivo,* confirming the efficacy of the imaging technique [10]. In this study, for the first time, OCT imaging with algorithm-based prediction was investigated intra-operatively and showed significant concordance (k = 0.92) with histological diagnosis of malignancies (100% specificity/sensitivity). The data also demonstrated that significant areas of clinically normal mucosa can harbor malignant lesions (n = 11). These occult malignant lesions could be detected accurately using intra-operative OCT imaging. The excellent concordance of OCT score and histology obtained suggested the possibility of using OCT as a surrogate for histopathology during intraoperative evaluation. Further, in an effort to improve the feasibility, the OCT device used in the study has been adapted and made portable to be used in the operation theatre (Supplementary Fig. 1A). The probe was also modified with long rigid rode with short ends that helped to take the image of different sites of oral cavity easily (Supplementary Fig. 1B). The accuracy along with its improved accessibility and portability designate this OCT device as a significant point of care tool for surgical margin delineation.

In an early detection setting, multiple imaging- based systems including algorithm-based dual model image analysis, autofluorescence, high-resolution microendoscopy (HRME), reflectance spectroscopy has showed good concordance with clinical detection of OPML [27,28]. The sensitivity of OCT in detecting dysplastic lesions around the tumor margins in

this study was significantly higher than clinical examination, with all the high-risk lesions [18] being detected by the OCT with statistically different scores. Significantly, all the OPMLs detected by clinical examination were diagnosed as dysplastic by OCT and subsequently by histology. However, low specificity (68%) in diagnosis of mild dysplastic lesions indicated that efficacy of OCT based diagnosis in differentiating between grades of dysplasia needs further research. Nevertheless, in the context of its utility in surgical margin demarcation, its accurate diagnosis of malignant and high-risk dysplastic lesions (moderate and severe dysplastic lesion) will have significant clinical utility [29].

A significant finding of this study was the ability of OCT based imaging to identify all malignant fields (n = 10) in tumor margin area and in the surgical margins (n = 1), which were clinically deemed normal. Evaluation of the OCT images of these sites shows loss of normal stratification of mucosa, while the histology shows discontinuous basement membrane and dysplastic sheets of cells in the stroma (Fig. 3). Microscopic examination, after total excision of tumor, showed submucosal extension of tumor in three patients. Additionally, one malignant site detected by OCT from outside surgical margin was also proven to be squamous cell carcinoma. The high-resolution visualization of deep structural morphologies achieved by OCT imaging in combination with the automated image analysis and scoring, improved the efficacy and reduced the subjectivity in the diagnosis. The accuracy in the diagnosis of sub-epithelial tumors indicated the potential of OCT for tumor margin delineation. Utilization of intra-operative OCT imaging in such tumors will enable more precise mapping of the tumor and tailoring the surgical margins.

As majority of oral cancer is caused by high-risk habits such as smoking, chewing of tobacco/areca nut and consumption of alcohol, the entire oral cavity mucosa can harbor dysplastic mucosa by the process of field cancerization [30–32]. The clinical significance of dysplastic lesions in the surgical margin is controversial, demonstrating both positive [33] and no correlation [34] with local recurrence. Field cancerization is an indicator of the extent of disease spread and increases the risk of disease recurrence and development of second primary tumors [31]. The alterations in the dysplastic field have been previously demarcated primarily in skin cancers by active tele thermography (ATT), narrow band imaging (NBI), HD-OCT and hyperspectral imaging enabling the detection of subclinical disease [35–38]. The field of cancerization in oral cancer has been interrogated by fluorescence imaging, dye-based techniques and biomarker-based studies [6,7,39], that showed capability to detect sub-clinical neoplastic fields, although a systematic mapping was not carried out. The mapping of the field around the tumor, as carried out in this study by OCT, indicated the presence of high-risk dysplastic sites in the surgical margin, at distances of over 1 cm from the margin (71%; n = 17/24; Supplementary Fig. 2). The high accuracy in delineating high-risk dysplastic sites at different distances from the tumor, suggested the feasibility of this non-invasive method to precisely map the field of cancerization. Field cancerization correlates to risk habits of the patients [31], however in this study this correlation could not be investigated as majority of the patients (n = 13/14) had risk habits. Nevertheless, the high incidence of dysplasia in the field (including the contralateral sites (69%)) detected in this study can be attributed to this high prevalence of risk habits.

Apart from evaluation of mucosal extent of tumor, assessment of deeper invasion of tumor is important to achieve three-dimensional tumor clearance during surgery. This study highlights the potential of OCT based imaging to delineate the mucosal and sub-mucosal extension of the tumor. However, considering the significance of deep margins as a prognosticator, the major limitation of the OCT, as applied in this study, was its inability to interrogate tissue over 2 mm depth. This is a limitation of OCT at its current stage of development.

Conclusion

Non-invasive and point-of-care methods that provide accurate diagnosis of the margin status intra-operatively are an invaluable adjunct to improving the efficacy of margin assessment. The present study demonstrates the accuracy of OCT-based imaging in identifying close margins that were undetected by visual examination; the detection of malignant clones in the surgical margins of patients that was deemed normal by clinical examination, was a significant finding. Additionally, the good concordance of OCT with histopathology for both malignant and high-risk lesions and its portability suggests a potential clinical application to map field cancerization around the tumor. Larger validation studies that include correlation with treatment outcome are mandatory prior to adaptation of the technology in the clinical practice, nevertheless, this study definitely outlines the significance and feasibility of OCT based surgical margin delineation.

Supplementary Material

Refer to Web version on PubMed Central for supplementary material.

Acknowledgments

Abbreviations:

OCT	optical coherence tomography
SCC	squamous cell carcinoma
OPML	oral potentially malignant lesion

References

[1]. Woolgar JA, Triantafyllou A. A histopathological appraisal of surgical margins in oral and oropharyngeal cancer resection specimens. Oral Oncol 2005;41:1034–43. [PubMed: 16129652]

[2]. Wong LS, McMahon J, Devine J, McLellan D, Thompson E, Farrow A, et al. Influence of close resection margins on local recurrence and disease-specific survival in oral and oropharyngeal carcinoma. Br J Oral Maxillofacial Surgery 2012;50:102–8.

[3]. Vikram B, Strong EW, Shah JP, Spiro R. Failure at the primary site following multimodality treatment in advanced head and neck cancer. Head Neck Surgery 1984;6:720–3. [PubMed: 6693287]

[4]. Mohiyuddin SMA, Padiyar BV, Suresh TN, Mohammadi K, Sagayaraj A, Merchant S, et al. Clinicopathological study of surgical margins in squamous cell carcinoma of buccal mucosa. World J Otorhinolaryngol - Head Neck Surgery 2016;2:17–21.

[5]. Gephardt GN, Zarbo RJ. Interinstitutional comparison of frozen section consultations. A college of American Pathologists Q-Probes study of 90,538 cases in 461 institutions. Arch Pathol Lab Med 1996;120:804–9. [PubMed: 9140284]

[6]. Kodama M, Khanal A, Habu M, Iwanaga K, Yoshioka I, Tanaka T, et al. Ultrasonography for intraoperative determination of tumor thickness and resection margin in tongue carcinomas. J Oral Maxillofacial Surgery: Off J Am Assoc Oral Maxillofacial Surgeons 2010;68:1746–52.

[7]. Poh CF, Zhang L, Anderson DW, Durham JS, Williams PM, Priddy RW, et al. Fluorescence visualization detection of field alterations in tumor margins of oral cancer patients. Clin Cancer Res: Off J Am Assoc Cancer Res 2006;12:6716–22.

[8]. Dakubo GD, Jakupciak JP, Birch-Machin MA, Parr RL. Clinical implications and utility of field cancerization. Cancer Cell Int 2007;7:2. [PubMed: 17362521]

[9]. Foo J, Leder K, Ryser MD. Multifocality and recurrence risk: a quantitative model of field cancerization. J Theor Biol 2014;355:170–84. [PubMed: 24735903]

[10]. Hamdoon Z, Jerjes W, McKenzie G, Jay A, Hopper C. Optical coherence tomography in the assessment of oral squamous cell carcinoma resection margins. Photodiagn Photodyn Ther 2016;13:211–7.

[11]. Shirani S, Kargahi N, Razavi SM, Homayoni S. Epithelial dysplasia in oral cavity. Iranian J Med Sci 2014;39:406–17.

[12]. Speight PM. Update on oral epithelial dysplasia and progression to cancer. Head Neck Pathol 2007;1:61–6. [PubMed: 20614284]

[13]. Heidari Andrew E, Sunny SP, James Bonney L, Tracie Lam, Tran Anne V, Junxiao Yu, et al. Optical coherence tomography as an oral cancer screening adjunct in a low resource setting. IEEE J Selected Topics Quant Electron 2018:99.

[14]. Tsai MT, Lee HC, Lee CK, Yu CH, Chen HM, Chiang CP, et al. Effective indicators for diagnosis of oral cancer using optical coherence tomography. Opt Express 2008;16:15847–62. [PubMed: 18825221]

[15]. Bujang MA, Adnan TH. Requirements for minimum sample size for sensitivity and specificity analysis. J Clin Diagnostic Res: JCDR 2016;10:YE01–6.

[16]. Alli PM, Ollayos CW, Thompson LD, Kapadia I, Butler DR, Williams BH, et al. Telecytology: intraobserver and interobserver reproducibility in the diagnosis of cervical-vaginal smears. Hum Pathol 2001;32:1318–22. [PubMed: 11774163]

[17]. Mun SK, Elsayed AM, Tohme WG, Wu YC. Teleradiology/telepathology requirements and implementation. J Med Syst 1995;19:153–64. [PubMed: 7602247]

[18]. Kujan O, Desai M, Sargent A, Bailey A, Turner A, Sloan P. Potential applications of oral brush cytology with liquid-based technology: results from a cohort of normal oral mucosa. Oral Oncol 2006;42:810–8. [PubMed: 16458571]

[19]. Amin MB, Edge S, Greene F, Byrd DR, Brookland RK, Washington MK, editors. AJCC Cancer Staging Manual. 8 edSpringer International Publishing; 2017.

[20]. Abbas SA, Ikram M, Tariq MU, Raheem A, Saeed J. Accuracy of frozen sections in oral cancer resections, an experience of a tertiary care hospital. JPMA J Pakistan Med Assoc 2017;67:806–9.

[21]. Erickson-Bhatt SJ, Nolan RM, Shemonski ND, Adie SG, Putney J, Darga D, et al. Real-time imaging of the resection bed using a handheld probe to reduce incidence of microscopic positive margins in cancer surgery. Cancer Res 2015;75:3706–12. [PubMed: 26374464]

[22]. Nguyen FT, Zysk AM, Chaney EJ, Kotynek JG, Oliphant UJ, Bellafiore FJ, et al. Intraoperative evaluation of breast tumor margins with optical coherence tomography. Cancer Res 2009;69:8790–6. [PubMed: 19910294]

[23]. Alawi SA, Kuck M, Wahrlich C, Batz S, McKenzie G, Fluhr JW, et al. Optical coherence tomography for presurgical margin assessment of non-melanoma skin cancer - a practical approach. Exp Dermatol 2013;22:547–51. [PubMed: 23879814]

[24]. Wessels R, van Beurden M, de Bruin DM, Faber DJ, Vincent AD, Sanders J, et al. The value of optical coherence tomography in determining surgical margins in squamous cell carcinoma of the vulva: a single-center prospective study. Int J Gynecol Cancer: Off J Int Gynecol Cancer Soc 2015;25:112–8.

[25]. Sahu A, Yelamos O, Iftimia N, Cordova M, Alessi-Fox C, Gill M, et al. Evaluation of a combined reflectance confocal microscopy-optical coherence tomography device for detection and depth assessment of basal cell carcinoma. JAMA Dermatol 2018;154:1175–83. [PubMed: 30140851]

[26]. Fei B, Lu G, Wang X, Zhang H, Little JV, Patel MR, et al. Label-free reflectance hyperspectral imaging for tumor margin assessment: a pilot study on surgical specimens of cancer patients. J Biomed Opt 2017;22:1–7.

[27]. Uthoff RD, Song B, Sunny S, Patrick S, Suresh A, Kolur T, et al. Point-of-care, smartphone-based, dual-modality, dual-view, oral cancer screening device with neural network classification for low-resource communities. PLoS ONE 2018;13:e0207493.

[28]. Yang EC, Schwarz RA, Lang AK, Bass N, Badaoui H, Vohra IS, et al. In vivo multimodal optical imaging: improved detection of oral dysplasia in low-risk oral mucosal lesions. Cancer Prevent Res 2018;11:465–76.

[29]. Jerjes W, Upile T, Conn B, Hamdoon Z, Betz CS, McKenzie G, et al. In vitro examination of suspicious oral lesions using optical coherence tomography. Br J Oral Maxillofacial Surgery 2010;48:18–25.

[30]. Sreedhar G, Narayanappa Sumalatha M, Shukla D. An overview of the risk factors associated with multiple oral premalignant lesions with a case report of extensive field cancerization in a female patient. Biomed Papers Med Faculty Univ Palacky, Olomouc, Czechoslovakia 2015;159:178–83.

[31]. Sathiasekar AC, Mathew DG, Jaish Lal MS, Arul Prakash AA, Goma Kumar KU. Oral field cancerization and its clinical implications in the management in potentially malignant disorders. J Pharm Bioallied Sci 2017;9:S23–5. [PubMed: 29284929]

[32]. Mohan M, Jagannathan N. Oral field cancerization: an update on current concepts. Oncol Rev 2014;8:244. [PubMed: 25992232]

[33]. Sopka DM, Li T, Lango MN, Mehra R, Liu JC, Burtness B, et al. Dysplasia at the margin? Investigating the case for subsequent therapy in 'low-risk' squamous cell carcinoma of the oral tongue. Oral Oncol 2013;49:1083–7. [PubMed: 24054332]

[34]. Kameyama JKAN. Evaluation of excisional biopsy for stage I and II squamous cell carcinoma of the oral cavity. Int J Clin Oncol 1998;3:317–22.

[35]. Laino L, Elia F, Desiderio F, Scarabello A, Sperduti I, Cota C, et al. The efficacy of a photolyase-based device on the cancerization field: a clinical and thermographic study. J Exp Clin Cancer Res: CR 2015;34:84. [PubMed: 26282842]

[36]. Tirelli G, Piovesana M, Gatto A, Tofanelli M, Biasotto M, Boscolo Nata F. Narrow band imaging in the intra-operative definition of resection margins in oral cavity and oropharyngeal cancer. Oral Oncol 2015;51:908–13. [PubMed: 26216339]

[37]. Neittaanmaki-Perttu N, Gronroos M, Tani T, Polonen I, Ranki A, Saksela O, et al. Detecting field cancerization using a hyperspectral imaging system. Lasers Surg Med 2013;45:410–7. [PubMed: 24037822]

[38]. Marneffe A, Suppa M, Miyamoto M, Del Marmol V, Boone M. Validation of a diagnostic algorithm for the discrimination of actinic keratosis from normal skin and squamous cell carcinoma by means of high-definition optical coherence tomography. Exp Dermatol 2016;25:684–7. [PubMed: 27095632]

[39]. Simple M, Suresh A, Das D, Kuriakose MA. Cancer stem cells and field cancerization of oral squamous cell carcinoma. Oral Oncol 2015;51:643–51. [PubMed: 25920765]

Fig. 1.

Study design. Clinical image (A) and schematic representation (B) of a patient with carcinoma of maxilla indicating the zones and the imaging sites. The tumor (T, Zone 1) is indicated along with the black outline representing the tumor margin (Zone 2). The imaging sites (A1 & B1) within zone 1 are also indicated. Blue outline represents the surgical-excision margin (Zone 3, imaging sites: A2 & B2), which is 1 cm away from clinical tumor margins and the yellow outline (Zone 4, imaging sites: A3 & B3) represents the region 1 cm away from the surgical margins (2 cm from the clinical tumor margin). OCT images using portable device (C) were captured intra-operatively after the surgeon marked the incision

line around the tumor. OCT images of 4 zones with OCT diagnosis and histology diagnosis in brackets is represented (D). Incisional biopsy was done with a 5 mm diameter punch at the point from which the OCT imaging was carried out (E). Histopathology diagnosis was compared to OCT and visual/palpation diagnosis. (For interpretation of the references to colour in this figure legend, the reader is referred to the web version of this article.)
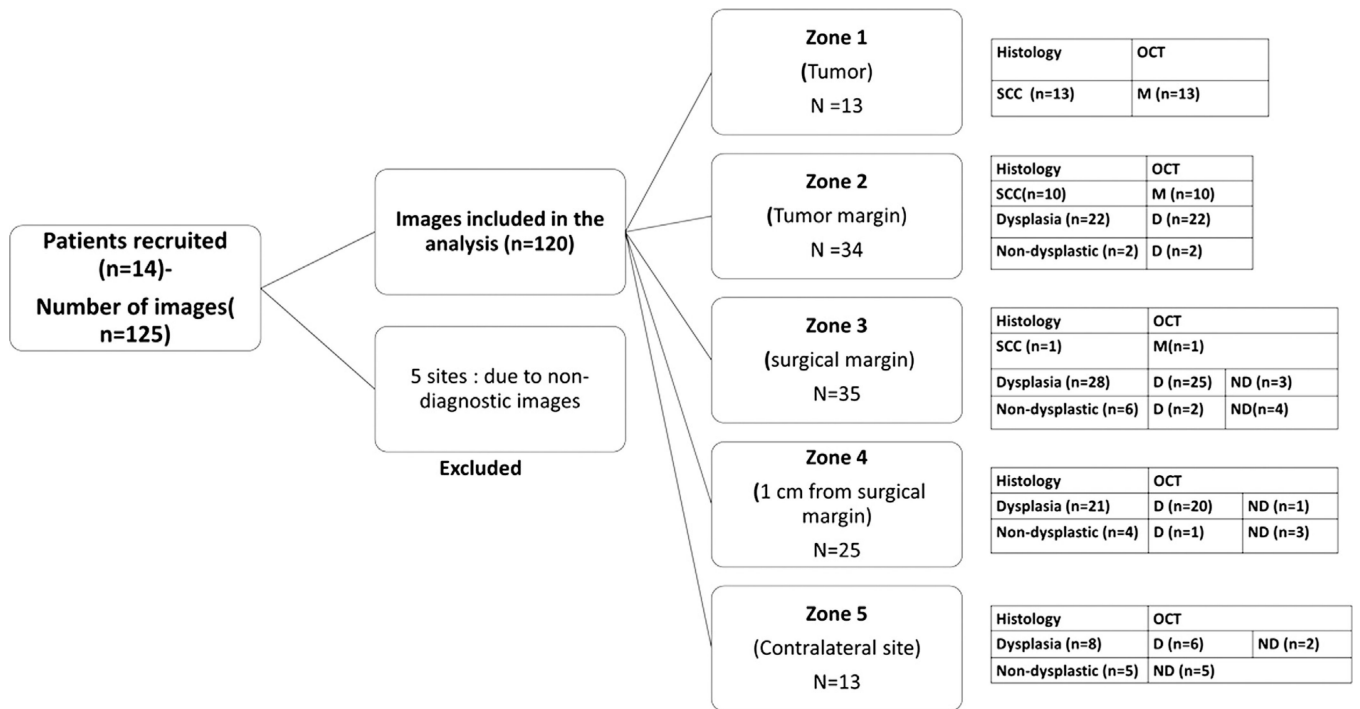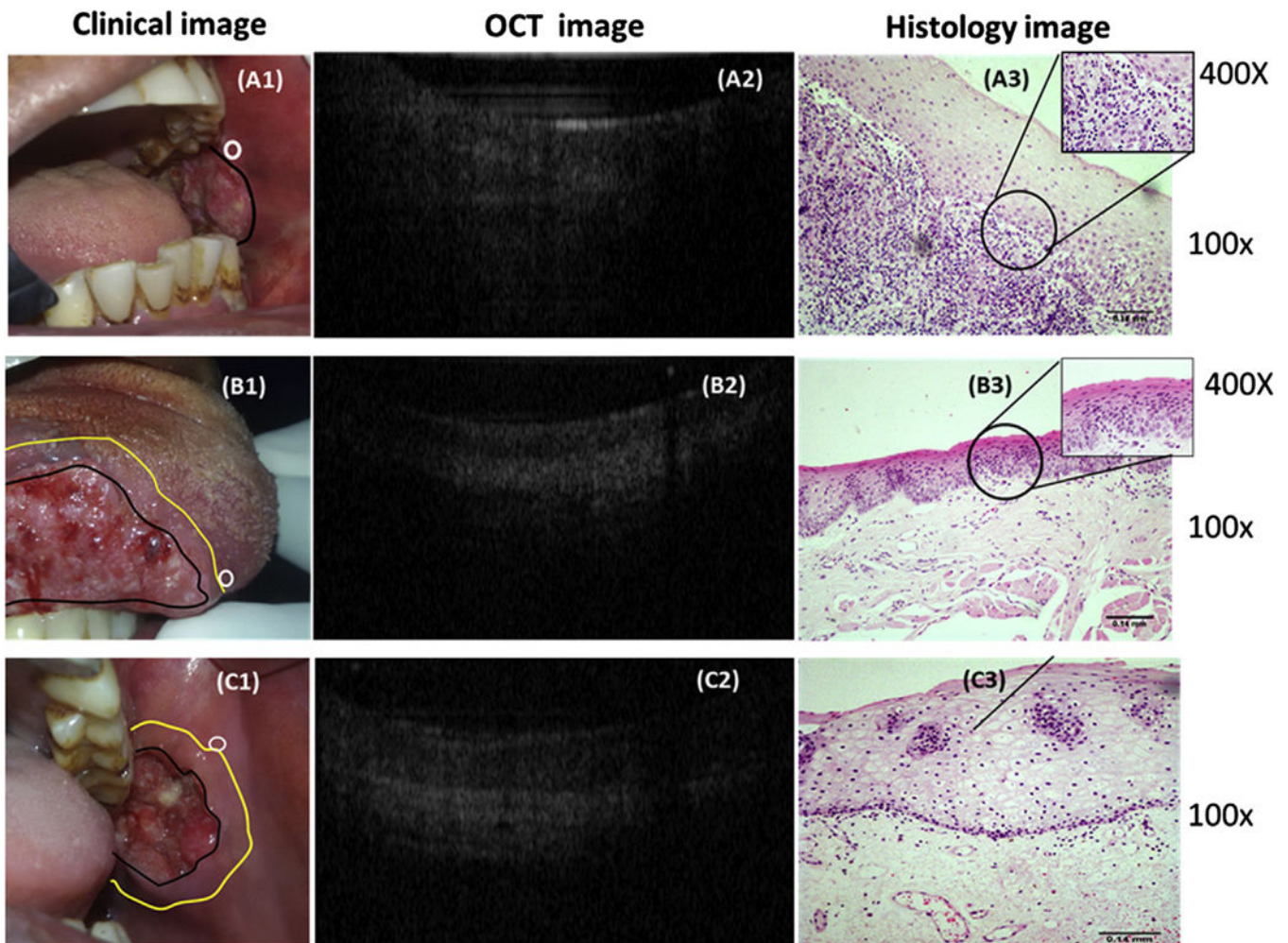
Fig. 2.
Study consort chart. Details of the patients, the total number of images captured and the distribution of patients' images in different zones according to histopathology and OCT diagnosis are provided. M=malignant, D=Dysplastic, ND=Non-Dysplastic, SCC- Squamous cell carcinoma.

Fig. 3.

Representative Clinical, OCT and Histology images of patients. (A1) Clinical image of a case of SCC of buccal mucosa; a clinically normal site (white circle) was chosen for OCT imaging and was diagnosed as malignancy by OCT (A2). The histology (**A3**-100×; inset 400×) shows loss of continuity of basement membrane with dysplastic epithelial islands in connective tissue suggesting squamous cell carcinoma. **(B1)** Clinical image of a patient with SCC of tongue; a clinically normal site outside the surgical margin (white circle) was imaged by OCT image **(B2)** and was diagnosed as dysplasia. Histopathology (100×) diagnosis was severe epithelial dysplasia **(B3)**. **(C1)** Clinical image of a case of SCC of buccal mucosa, a clinically normal (white circle) outside the surgical margin was diagnosed by OCT **(C2)** and histology **(C3)** (100×) as non-dysplastic.
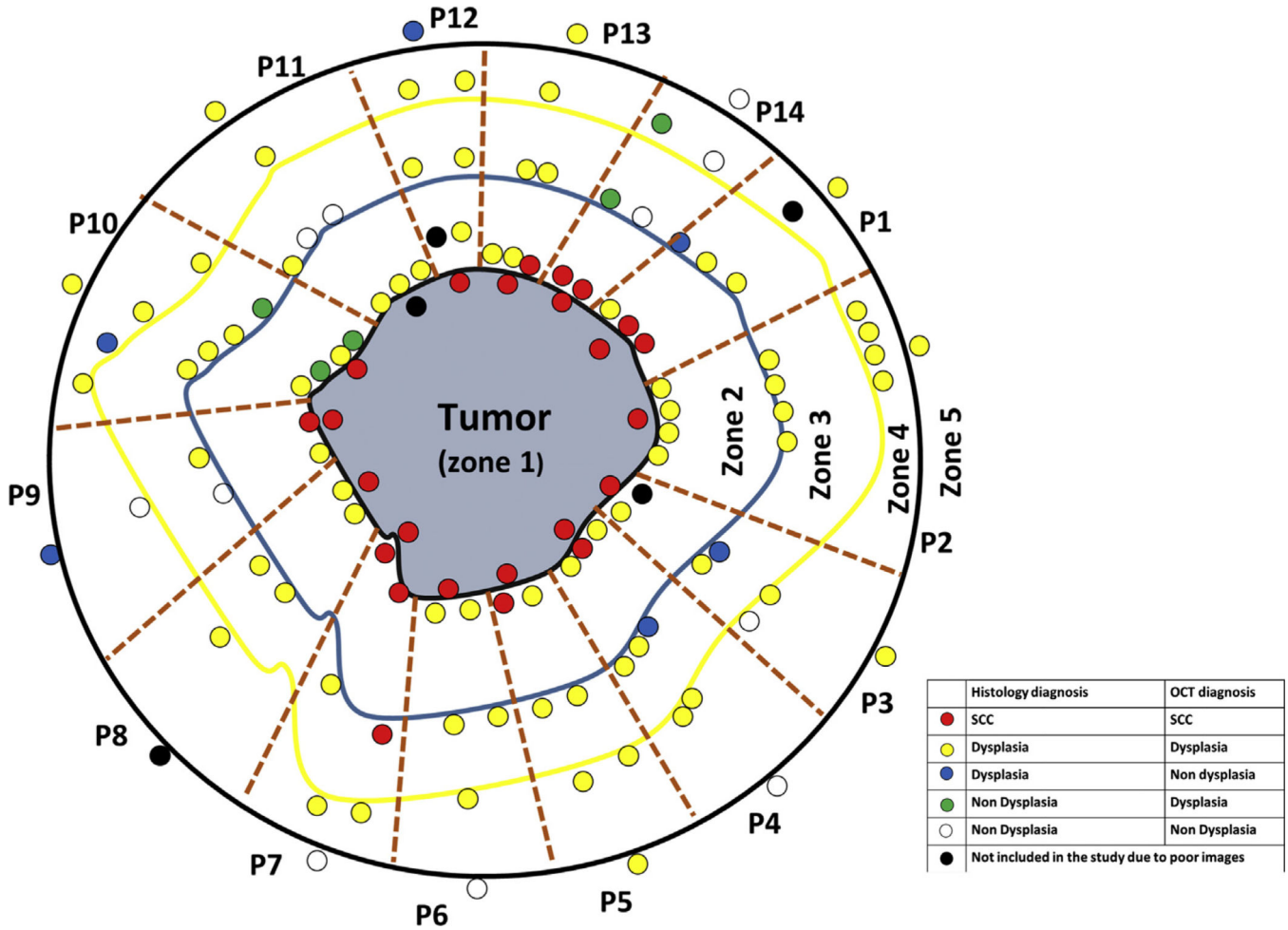
Fig. 4.
Comparative diagnosis of all images captured from different zones of all patients. Each block (brown dotted lines) represents each patient (n = 14). The central grey area represents the tumor (zone 1) with black outline representing the margin (Zone 2), blue (Zone 3) and yellow outline (Zone 4) representing the surgical margin and > 1 cm from surgical margin respectively. Each small circle represents the captured sites, with the colors indicating the comparative diagnosis. The circles around the outside of the black outline (zone 5) represents imaged sites from contralateral sites. Red, yellow and white represent concordant diagnosis of SCC, dysplasia and non-dysplasia, while blue and green colored small circles represent false negative and false positive respectively in diagnosis of dysplasia. (P = Patient) (For interpretation of the references to colour in this figure legend, the reader is referred to the web version of this article.)
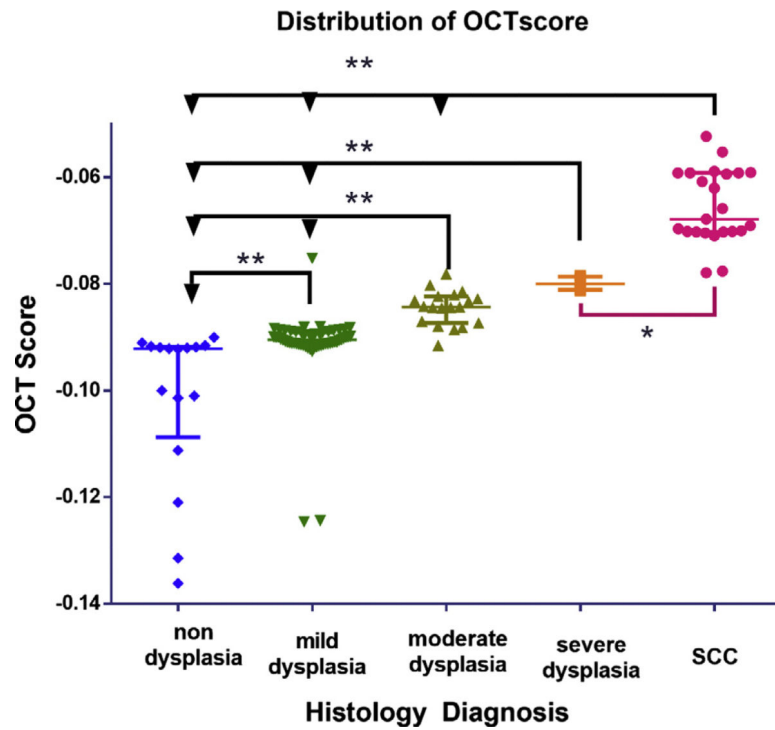
Fig. 5.

Distribution of OCT score according to histology diagnosis. Box whisker plot indicating the OCT score of individual sites classified according to histopathology diagnosis. Kruskal wallis test show significant variance within the groups (p < 0.005) and no significant difference between moderate and severe dysplasia. The data shows median and interquartile range (**p < 0.005, * p < 0.05).

Table 1:

Demographic data of patients and number of images from different sites.

Patient	Age	Size of tumor	Site	Number of images				
				zone 1	zone 2	zone 3	zone 4	zone 5
1	52	T2	Maxillary GBS (L)	1	3	3	NA	1
2	49	T4b	Buccal mucosa (L)	1	4	4	4	1
3	65	T4b	Buccal mucosa (L)	1	1	2	2	1
4	39	T4b	Buccal mucosa (R)	1	3	3	2	1
5	52	T2	Buccal mucosa (L)	1	2	2	2	1
6	47	T4b	Buccal mucosa (L)	1	2	2	1	1
7	78	T2	Retro molar trigone (L)	1	2	2	2	1
8	70	T4a	Maxillary alveolus (R)	1	2	2	1	NA
9	58	T3	Maxillary GBS (L)	1	2	2	1	1
10	55	T4b	Mandibular alveolus (L)	1	4	4	4	1
11	55	T1	Tongue	NA	3	3	1	1
12	71	T4a	Mandibular alveolus (R)	1	1	2	2	1
13	42	T2	Tongue	1	3	2	1	1
14	42	T2	Buccal mucosa (L)	1	2	2	2	1

Table 2:

Sensitivity, specificity (with 95% confidence interval) and accuracy of OCT and visual diagnosis in detection of malignancy and dysplasia in the different zones (zone 1–5).

Method	Sensitivity	Specificity	Accuracy
OCT – malignancy (Zone 1&2)	100 (85.2–100)	100 (85.8–100)	100
Visual – Malignancy (Zone 1 & 2)	56.5 (34.5–76.9)	100 (96.3–100)	78.7
OCT- Dysplasia (zone 2–5)	92.5 (84.4–97.2)	68.8 (41.3–88.9)	88.5